

Periodic image effects in dislocation modelling

WEI CAI^{†‡§}, VASILY V. BULATOB[†], JINPENG CHANG[‡], JU LI[‡],
and SIDNEY YIP[‡]

[†] Lawrence Livermore National Laboratory, University of California, Livermore,
California 94550, USA

[‡] Department of Nuclear Engineering, Massachusetts Institute of Technology,
Cambridge, Massachusetts 02139, USA

[Received 9 May 2002 and accepted 4 October 2002]

ABSTRACT

The use of periodic boundary conditions for modelling crystal dislocations is predicated on one's ability to handle the inevitable image effects. This communication deals with an often overlooked mathematical subtlety involved in dealing with the periodic dislocation arrays, that is *conditional convergence* of the lattice sums of image fields. By analysing the origin of conditional convergence and the numerical artefacts associated with it, we establish a mathematically consistent and numerically efficient procedure for regularization of the lattice sums and the corresponding image fields. The regularized solutions are free from the artefacts caused by conditional convergence and regain periodicity and translational invariance of the periodic supercells. Unlike the other existing methods, our approach is applicable to general anisotropic elasticity and arbitrary dislocation arrangements. The capabilities of this general methodology are demonstrated by application to a variety of situations encountered in atomistic and continuum modelling of crystal dislocations. The applications include introduction of dislocations in the periodic supercell for subsequent atomistic simulations, atomistic calculations of the core energies and the Peierls stress and continuum dislocation dynamics simulations in three dimensions.

§1. INTRODUCTION

Solid-state theory owes much of its success to constructive uses of the Bloch's theorem (Kittel 1976). The latter applies to systems that are either naturally periodic or made periodic by replication of the computational *supercell* throughout space. The principal advantage of periodic boundary conditions (PBCs) for modelling crystal defects is that they eliminate surfaces and preserve translational invariance, the fundamental property of the crystal lattice. However, the advantages of using PBC often come at a price: instead of a single defect of interest, the periodic closure of the system introduces an infinite array of defects whose interaction may distort the computed properties of the defect. The unwanted effects of periodicity can be large for the defects producing long-range fields, such as electrostatic fields of charged defects or elastic fields of lattice dislocations. In order to extract properties of indi-

§ Author for correspondence. Email: caiwei@llnl.gov.

vidual defects from the properties of periodic arrays, such spurious contributions should be accurately evaluated.

The effects of PBCs are usually considered by embedding the simulation cell in an infinite and periodic array of image supercells that are exact replicas of the primary cell. In this context, the elastic fields of the defect in PBCs can be constructed by superimposing the fields produced by the defect in the primary simulation cell and image fields of its periodic replicas. Similarly, the superfluous image energy can be computed by summing the interaction energies between the primary and image defects. Unfortunately, in some important cases the image sum is only *conditionally convergent*. The Riemann series theorem states that, by regrouping the terms, it is possible to make such sums converge to an arbitrarily chosen limit (Whittaker and Watson 1958). A similar problem arises in summing electrostatic energy in ionic crystals, known as the Madelung summation (de Leeuw 1980, Smith 1981, Borwein *et al.* 1985). If such is the case, a straightforward summation using some naïve grouping of terms will fail to provide a definite answer of the image effect. For the specific case of computing dislocation image energies in PBCs, the existing techniques have been limited to isotropic elasticity or to special dislocation arrangements in the periodic supercell (Gulluoglu *et al.* 1989, Wang and LeSar 1995, Blase *et al.* 2000, Ismail-Beigi and Arias 2000). In this paper, we develop a robust method that is applicable to general anisotropic elasticity and arbitrary dislocation configurations in periodic supercells. The method follows from the observation that, when summing the fields produced by an infinite periodic array of sources, conditional convergence and the breaking of periodicity are related. By fixing the latter, the conditional convergent sum is regularized to its physical solution. We then establish a connection between the conditional convergence of image energy and that of the potential field of dislocations. The image energy is regularized by subtracting the non-periodic component of the potential field, which is conveniently carried out by introducing a set of probing ‘ghost’ dislocations that interact with image dislocations. We present several key applications selected to demonstrate the power and applicability of the method to modelling dislocations in PBCs.

We begin with a discussion of the origin of conditional convergence in §2. In §3.1, we show that spurious fields produced by conditionally convergent sums contain low-order polynomials that violate periodicity and that the physical solutions can be recovered by measuring and subtracting such spurious field components. In §3.2, we develop a method for computing the image energy based on the work of insertion of a dislocation dipole into the periodic supercell (Cai 2001). The solution provides a correction term that, once subtracted from the lattice sum, makes it independent of the choice of the summation sequence. A detailed derivation is given in appendix A and an alternative solution based on the elastic Green’s function is given in appendix B. In §4, four applications of the new method are presented. Firstly, we apply the method to specify initial atomic configurations correctly for dislocation simulations in the periodic supercells. Secondly, we examine the energetics of dislocations in silicon and find an excellent match between our method’s predictions and the data from direct atomistic simulations. Based on this agreement, we extract dislocation core energies from atomistic simulations without any adjustable parameters (Cai *et al.* 2001). Thirdly, we use the new method for designing optimal supercell geometries that minimize image interactions and make it possible to compute dislocation Peierls stress with high accuracy. Fourthly, the method is used to develop an efficient procedure for computing periodic image interactions in

three-dimensional dislocation dynamics simulations in PBCs (Bulatov *et al.* 2001). Finally, § 5 summarizes the discussion.

§ 2. THE PROBLEM OF CONDITIONAL CONVERGENCE

2.1. Conditional convergence of the elastic fields

Conditional convergence of the lattice sums is a consequence of the long-range character of the elastic fields of dislocations. Consider a dislocation dipole in a simulation supercell with periodic vectors \mathbf{c}_1 , \mathbf{c}_2 and \mathbf{c}_3 , as shown in figure 1. Two dislocation lines, with Burgers vectors \mathbf{b} and $-\mathbf{b}$, are parallel to \mathbf{c}_3 and separated by \mathbf{a} . Let us construct the stress field in this PBC cell by summing the individual contributions from the image dipoles in the periodic lattice:

$$\sigma_{ij}^{\text{sum}}(\mathbf{r}) \equiv \sum_{\mathbf{R}} \sigma_{ij}^{\text{dipole}}(\mathbf{r} - \mathbf{R}), \tag{1}$$

where $\sigma_{ij}^{\text{dipole}}(\mathbf{r} - \mathbf{R})$ is the stress field of a dipole at position \mathbf{R} with respect to the primary dipole. The summation runs over two-dimensional lattice $\mathbf{R} = n_1\mathbf{c}_1 + n_2\mathbf{c}_2$ (n_1 and n_2 are integers) specifying positions of the image dipoles with respect to the primary dipole.

The stress field of a straight dislocation (Hirth and Lothe 1982, p. 59) behaves as R^{-1} at large R (in two dimensions) while the stress field of a dislocation dipole decays as R^{-2} . Therefore, the sum of stress fields by their absolute values at any point \mathbf{r} diverges logarithmically:

$$\sum_{\mathbf{R}} |\sigma_{ij}^{\text{dipole}}(\mathbf{r} - \mathbf{R})| \propto \int^{\infty} dR 2\pi R \frac{1}{R^2} \propto \int^{\infty} dR \frac{1}{R} \sim \infty. \tag{2}$$

This means that the summation in equation (1) is not *absolutely convergent*. On the other hand, in practice the sum in equation (1) does converge, owing to partial cancellation of terms with the opposite signs. However, because this sum is not *absolutely convergent*, as was shown by Riemann (see Whittaker and Watson (1958)), one can make it converge conditionally to virtually any value, by selecting

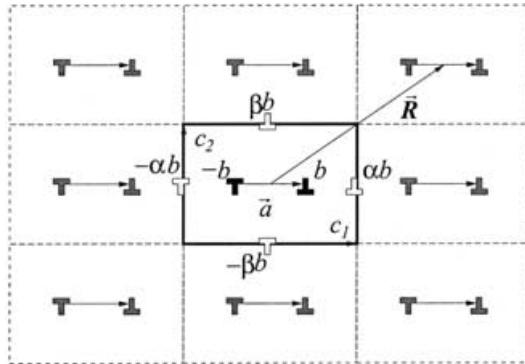


Figure 1. A periodic simulation cell (solid rectangle) of box vectors \mathbf{c}_1 , \mathbf{c}_2 , \mathbf{c}_3 (out of plane), containing a dislocation dipole under PBCs. The two dislocations have Burgers vector $\pm\mathbf{b}$ and are separated by \mathbf{a} . Image dipoles are illustrated in grey and ‘ghost’ dislocations introduced to facilitate image energy calculation are plotted in white.

the order in which the terms are summed or by choosing the limit of truncation. For example, summation of the interaction terms by expanding concentric circles converges to a different limit than a summation by expanding rectangles. This behaviour of *conditional convergence* makes the straightforward (naïve) summation invalid for providing a definite solution for the true stress field in the periodic cell.

Obviously the same problem occurs in displacement field since its derivative, strain, is related to stress by the elastic constants. Another case worth mentioning is dislocation dynamics simulations in three dimensions where dislocations are discretized into short line segments interacting with each other through their stress fields (Devincre and Kubin 1997, Zbib *et al.* 1998, Schwarz 1999, Ghoniem *et al.* 2000). Since the stress of a short dislocation segment behaves as R^{-2} , the infinite sum of stress contributions from its image segments, now in three dimensions, is conditionally convergent again. In order to take full advantage of PBCs for dislocation simulations, these and other similar difficulties have to be resolved.

2.2. Conditional convergence of the interaction energy

Let us consider an atomistic configuration of dislocation dipole in a periodic supercell (figure 1). If the initial atomic configuration is chosen appropriately (see §4.1), subsequent relaxation brings the system's energy to a local minimum. Let us define E_{atm} as the energy in excess of the energy of a perfect lattice with the same number of atoms. The problem of interest is to extract dislocation core energy from the 'raw' simulation data E_{atm} that is sure to contain yet unknown contribution from the image interactions.

In the limit of $c_1/a, c_2/a \rightarrow \infty$, E_{atm} must converge to a physical quantity E_{dipole} —the energy of an isolated dislocation dipole in an infinite lattice. However, in practice, especially because of the need to limit the number of atoms in *ab initio* calculations, the cell dimensions c_1 and c_2 are comparable with a . Then, it becomes necessary to account for an additional energy of the periodic image interactions E_{img} , as in

$$E_{\text{atm}} = E_{\text{dipole}} + E_{\text{img}}. \quad (3)$$

In turn, the dipole energy itself can be separated into two contributions: one associated with the core regions, and the other associated with the long range elastic fields of the two dislocations:

$$E_{\text{dipole}} = 2E_{\text{core}}(r_c) + E_{\text{prm}}(r_c), \quad (4)$$

where $E_{\text{core}}(r_c)$ is the dislocation core energy, $E_{\text{prm}}(r_c)$ is the elastic energy of the dislocation dipole and r_c is a cut-off radius introduced to avoid the singularity of the elastic energy in the core. For example, elastic energy (per unit length) of a dipole of two parallel screw dislocations in an infinite isotropic solid with shear modulus μ is

$$E_{\text{prm}}(r_c) = \frac{\mu b^2}{2\pi} \ln \left(\frac{a}{r_c} \right). \quad (5)$$

Here, because of the arbitrariness of r_c , E_{core} is not a physical quantity in the sense that it cannot be defined or measured independently. To make this parameter meaningful, a reference radius r_c must be specified. Given this partitioning, E_{atm} can be written as follows:

$$E_{\text{atm}} = 2E_{\text{core}}(r_c) + E_{\text{prm}}(r_c) + E_{\text{img}}.$$

Here, $E_{\text{prm}}(r_c)$ and E_{img} are two parts of elastic energy, one of which (E_{img}) is due to the image interactions. Thus, the effort of extracting E_{core} from E_{atm} reduces to calculating E_{img} .

Intuitively, one writes E_{img} as a sum of interaction energies between the (primary) dislocation dipole and its periodic images

$$E'_{\text{img}} = \frac{1}{2} \sum'_{\mathbf{R}} E_{\text{dd}}(\mathbf{R}), \quad (6)$$

where $E_{\text{dd}}(\mathbf{R})$ is the interaction energy of two dipoles separated by vector \mathbf{R} and the summation runs over two-dimensional lattice $\mathbf{R} = n_1 \mathbf{c}_1 + n_2 \mathbf{c}_2$ (n_1 and n_2 are integers) specifying positions of the image dipoles with respect to the primary dipole. The factor $\frac{1}{2}$ appears because only half the interaction energy term is ascribed to the primary cell whereas the other half belongs to the image cell. The prime in \sum' means that the singular term ($n_1 = n_2 = 0$) is excluded from summation and the prime in E'_{img} symbolizes that the image energy is not yet well defined owing to the conditional convergence of the lattice sum.

Let us consider, as an example, a screw dislocation dipole in an isotropic solid so that the dipole–dipole interaction term becomes

$$\begin{aligned} E_{\text{dd}}(\mathbf{R}) &= \frac{\mu b^2}{2\pi} \ln \left(\frac{|\mathbf{R} + \mathbf{a}| \cdot |\mathbf{R} - \mathbf{a}|}{|\mathbf{R}|^2} \right) \\ &\approx -\frac{\mu b^2}{2\pi} \frac{a^2}{R^2} \cos(2\theta) \\ &\propto R^{-2} \quad \text{for } R \gg a, \end{aligned} \quad (7)$$

$$(8)$$

where $\theta = \arccos[(\mathbf{a} \cdot \mathbf{R})/aR]$. Since $|E_{\text{dd}}(\mathbf{R})| \propto R^{-2}$ for all dislocation dipoles, the sum of the absolute values of such interaction terms diverges logarithmically, similar to the stress fields in §2.1. This means that the summation in equation (6) is not absolutely convergent. On the other hand, as was observed in all previous communications (Arias and Joannopoulos 1994, Hansen *et al.* 1995, Lehto and Heggie 1999, Blase *et al.* 2000), the sum in equation (6) does converge, evidently owing to a partial cancellation of terms with the opposite signs. However, this behaviour of conditional convergence makes it virtually impossible to obtain the true value of E_{img} from a straightforward (naïve) summation in equation (6). The earlier reports (Arias and Joannopoulos 1994, Hansen *et al.* 1995) dealing with the dislocation image sums in PBCs ignored the issue of conditional convergence and did not specify the order of summation. The results of such calculations are arbitrary and the reported values of the core energies are nearly certainly incorrect.

§3. REGULARIZATION OF THE CONDITIONALLY CONVERGENT SUMS

3.1. Regularization of elastic fields

A physically meaningful solution for the total elastic field of a periodic array of field sources should be periodic itself with the exact periodicity of the supercell. It turns out that the naïve superposition of image terms not only is conditionally convergent but also produces fields that are, as a rule, non-periodic. This suggests that the non-uniqueness of the conditionally convergent sums and the observed spurious breaking of translational periodicity are closely related and, if one issue

is resolved, another will be corrected too. Generally speaking, if the field from a single source behaves as $1/r^m$ at large r , then the lattice sums of the derivatives of certain order and above should be *absolutely convergent*. Conversely, the conditionally convergent part of the field should be representable by a low-order polynomial in \mathbf{r} , such as a constant (e.g. ϕ^0) or a linear term (e.g. $\phi^0 + \mathbf{g} \cdot \mathbf{r}$), depending on m and the lattice dimensionality.

A simple recipe to reconstruct the fields from a conditionally convergent series is first to go ahead and to compute a lattice sum of the field sources following some arbitrarily selected grouping of terms. The second step is to measure and subtract the spurious part of the field that appears owing to conditional convergence. In this section, we describe this approach using the potential energy field of dislocations as an example. The solution given here will be utilized in the following § for regularization of the image energy. A similar method is used in §4.1 to correct dislocation displacement fields, which is useful for setting up atomistic simulations of dislocations in PBCs. In §4.4, we apply the method to account for the image stress fields in three-dimensional dislocation dynamics simulations in PBCs.

In this § we consider, as an example, a scalar potential field $\phi(\mathbf{r})$ defined as the interaction energy (per unit length) between the periodic dipole array and a test dislocation \mathbf{b} at position \mathbf{r} . Similar to the stress field in equation (1), $\phi(\mathbf{r})$ is a superposition of the potential fields of individual dipoles. Consider, as an example, a dipole of screw dislocations in an elastically isotropic solid located at $\mathbf{a}/2$ and $-\mathbf{a}/2$ in a periodic supercell. The potential field of the image dipoles is

$$\phi(\mathbf{r}) = \sum_{\mathbf{R}} \frac{\mu b^2}{2\pi} \ln \left(\frac{|\mathbf{r} - (\mathbf{R} - \mathbf{a}/2)|}{|\mathbf{r} - (\mathbf{R} + \mathbf{a}/2)|} \right). \quad (9)$$

The individual terms in equation (9) are proportional to $1/R$ at large R ; hence their sum $\phi(\mathbf{r})$ is not absolutely convergent. Similarly, the sum of the first spatial derivatives of the field contributions $\partial_i \phi(\mathbf{r})$ ($i = 1, 2$) is conditionally convergent since the individual terms are proportional to $1/R^2$. Taking it one step further, the second derivatives $\partial_i \partial_j \phi(\mathbf{r})$ ($i, j = 1, 2$) are proportional to $1/R^3$ and their sum will converge absolutely to the same limit regardless of the order of summation.

We now prove that an absolutely convergent sum of fields from a periodic array of sources converges to a field $h(\mathbf{r})$ (e.g. $\partial_i \partial_j \phi(\mathbf{r})$) that is also periodic. Consider a partial sum over a large summation domain Ω of an arbitrary shape, say, a circle as in figure 2. Assume also that Ω_1 is the same as Ω , only shifted by \mathbf{c}_1 . By periodicity, the partial lattice sum $h^\Omega(\mathbf{r})$ over domain Ω is identical with the partial lattice sum $h^{\Omega_1}(\mathbf{r} + \mathbf{c}_1)$ over the shifted domain Ω_1 . What we need to prove, however, is that these two partial sums converge to the same limit when summed over the *same domain*. Consider a common region Ω_0 that lies in the intersection of Ω and Ω_1 . Noting that an absolutely convergent sum converges to the same limit no matter how it is truncated, we have

$$\lim_{\Omega_0 \rightarrow \infty} [h^\Omega(\mathbf{r})] = \lim_{\Omega_0 \rightarrow \infty} [h^{\Omega_1}(\mathbf{r})] = h(\mathbf{r}), \quad (10)$$

$$\lim_{\Omega_0 \rightarrow \infty} [h^{\Omega_1}(\mathbf{r} + \mathbf{c}_1)] = \lim_{\Omega_1 \rightarrow \infty} [h^{\Omega_1}(\mathbf{r} + \mathbf{c}_1)] = h(\mathbf{r} + \mathbf{c}_1). \quad (11)$$

Since $h^\Omega(\mathbf{r}) \equiv h^{\Omega_1}(\mathbf{r} + \mathbf{c}_1)$, we prove that $h(\mathbf{r}) = h(\mathbf{r} + \mathbf{c}_1)$ and, similarly, $h(\mathbf{r}) = h(\mathbf{r} + \mathbf{c}_2)$.

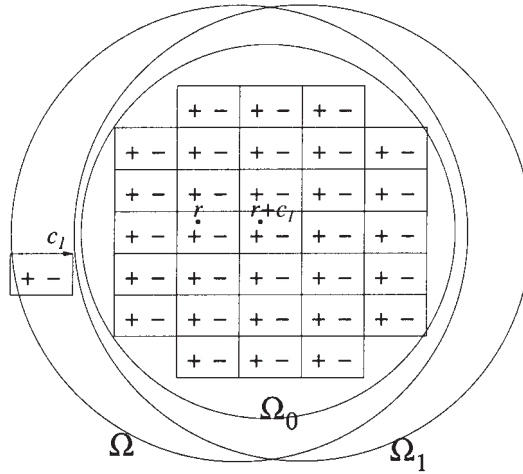


Figure 2. To prove that an absolutely convergent sum of fields from a periodic array of sources is periodic, we consider two field points \mathbf{r} and $\mathbf{r} + \mathbf{c}_1$, where \mathbf{c}_1 is a lattice repeat vector. Here Ω is an arbitrary but large summation domain and Ω_1 is obtained by shifting Ω by \mathbf{c}_1 . Ω_0 lies in the intersection of Ω and Ω_1 .

For the field $\phi(\mathbf{r})$ that is *not* absolutely convergent and, hence, may *not* be periodic, we define

$$\phi(\mathbf{r}) = \phi^{\text{PBC}}(\mathbf{r}) + \Delta\phi(\mathbf{r}), \tag{12}$$

where $\phi^{\text{PBC}}(\mathbf{r})$ is the invariant periodic component and $\Delta\phi(\mathbf{r})$ is the non-periodic spurious part of the field that may be different for different summation procedures. Given that $\partial_i\partial_j\phi(\mathbf{r})$ is absolutely convergent and, hence, periodic, the non-periodic part of the conditionally convergent field is, by integration,

$$\Delta\phi(\mathbf{r}) = \mathbf{g} \cdot \mathbf{r} + \phi^0, \tag{13}$$

where ϕ^0 is an integration constant and \mathbf{g} is a constant vector. These two terms are artefacts of the conditional convergence and should be subtracted in order to obtain a unique periodic solution for the potential field.

Because $\phi^{\text{PBC}}(\mathbf{r}) = \phi^{\text{PBC}}(\mathbf{r} + \mathbf{c}_{1,2})$, to measure the slope \mathbf{g} of the spurious field one can use, for example,

$$\begin{aligned} \mathbf{g} \cdot \mathbf{c}_1 &= \phi(\mathbf{r}_1 + \mathbf{c}_1) - \phi(\mathbf{r}_1), \\ \mathbf{g} \cdot \mathbf{c}_2 &= \phi(\mathbf{r}_2 + \mathbf{c}_2) - \phi(\mathbf{r}_2), \end{aligned} \tag{14}$$

for arbitrary \mathbf{r}_1 and \mathbf{r}_2 . In other words, the average slope \mathbf{g} of the potential field can simply be ‘measured’ by comparing field values in two pairs of points separated by lattice repeat vectors. In two dimensions, two measurements are sufficient to determine \mathbf{g} . The constant ϕ^0 is immaterial and can be eliminated by redefining the reference point of the potential energy. The desired periodic solution is then recovered by subtracting $\mathbf{g} \cdot \mathbf{r}$ from the non-periodic, conditionally convergent field $\phi(\mathbf{r})$.

3.2. Regularization of the image energy

Now let us consider the image energy as introduced in §2.2. The arbitrariness of E'_{img} in equation (6) associated with conditional convergence is a numerical artefact. This follows from the fact that, for a given size of the dipole, both E_{atm} and E_{dipole} in equation (3) are two well-defined quantities. The first of these, E_{atm} , can be ‘measured’ directly in an atomistic calculation for any given size and shape of the supercell. The second quantity, E_{dipole} , can be obtained without any recourse to the lattice sums, as a limit of E_{atm} computed in increasingly large supercells. Hence, their difference, E_{img} , should be a well-defined quantity too. Several methods have been proposed so far to circumvent the conditional convergence problem by regularization of the image sums. Edge dislocations, in particular, can be grouped into infinite walls whose interaction is short-ranged and thus absolutely convergent (Wang and LeSar 1995). Alternatively, a Ewald-like method has been used for periodic arrays of screw dislocations (Ismail-Beigi and Arias 2000). So far, applicability of these two methods has been limited by the common assumption of isotropic elasticity. The recipe of grouping dislocations into quadrupoles can be used in conjunction with anisotropic elasticity, but it requires special dislocation arrangements (Bigger *et al.* 1992, Wolf 1992, V. V. Bulatov 1998, unpublished). A general solution is needed that is sufficiently robust to handle anisotropic elasticity as well as arbitrary dislocation configurations.

In this section, we describe a solution that meets these requirements and some ideas used for its derivation. Only a brief outline of the derivation is presented here while the details are given in appendix A.

Firstly, by considering the reversible work of introducing a dislocation dipole in a periodic elastic solid, we find that the total elastic energy of a dislocation dipole under PBCs can be expressed in terms of the stress field $\sigma_{ij}(\mathbf{r})$ as (see §A.1),

$$E_{\text{el}} = -\frac{1}{2} \int dA_j b_i \sigma_{ij}^0(\mathbf{r}) + \frac{1}{2} S \bar{\sigma}^2 V, \quad (15)$$

where $\bar{\sigma} \equiv \langle \sigma(\mathbf{r}) \rangle_V$ is the average stress, and $\sigma^0(\mathbf{r}) \equiv \sigma(\mathbf{r}) - \bar{\sigma}$ is the variation in the stress field with zero average.

In an attempt to relate equation (15) to the naïve image sum in equation (6), we write $\sigma^0(\mathbf{r})$ as

$$\sigma_{ij}^0(\mathbf{r}) = \sigma_{ij}^{\text{sum}}(\mathbf{r}) - \sigma_{ij}^{\text{err}}, \quad (16)$$

where $\sigma_{ij}^{\text{sum}}(\mathbf{r})$ is defined in equation (1) and $\sigma_{ij}^{\text{err}} \equiv \langle \sigma_{ij}^{\text{sum}}(\mathbf{r}) \rangle_V$ is its volume average. As shown in §A.1, assuming that the average stress $\bar{\sigma}$ in the supercell is relaxed to zero, this leads to an expression for the image energy that includes the naïve image interaction sum plus a correction term:

$$E_{\text{img}} = \frac{1}{2} \sum_R' E_{\text{dd}}(\mathbf{R}) + \frac{1}{2} A_j b_i \sigma_{ij}^{\text{err}}. \quad (17)$$

The σ_{ij}^{err} term is the spurious volume average of the stress field in the supercell which is also the derivative of the spurious non-periodic part of the potential field computed through equations (13) and (14) in §3.1. By subtracting this term, periodicity of the potential field as well as the absolute convergence of the image energy are restored. Operationally, this is done by inserting ‘ghost’ dislocations at the cell boundaries and rewriting the correction term as the sum of interaction energies between ‘ghost’ and image dislocations. As shown in figure 1, it is sufficient to insert

four ‘ghost’ dislocations $\alpha\mathbf{b}$, $-\alpha\mathbf{b}$ and $\beta\mathbf{b}$ and $-\beta\mathbf{b}$, so that $\alpha\mathbf{b}$, $-\alpha\mathbf{b}$ are separated by \mathbf{c}_1 , $\beta\mathbf{b}$ and $-\beta\mathbf{b}$ are separated by \mathbf{c}_2 , and α and β are such that $\mathbf{a} = \alpha\mathbf{c}_1 + \beta\mathbf{c}_2$. Define $E_{\text{dg}}(\mathbf{R})$ as the interaction energy between an image dipole offset from the primary dipole by \mathbf{R} with the ‘ghost’ dislocations. The resulting corrected, or regularized, sum is

$$E_{\text{img}} = \frac{1}{2} \sum_R' E_{\text{dd}}(\mathbf{R}) - \frac{1}{2} \sum_R E_{\text{dg}}(\mathbf{R}) \tag{18}$$

$$= \frac{1}{2} \sum_R' [E_{\text{dd}}(\mathbf{R}) - E_{\text{dg}}(\mathbf{R})] - \frac{1}{2} E_{\text{dg}}(\mathbf{R} = 0), \tag{19}$$

where the sum \sum includes $\mathbf{R} = \mathbf{0}$ (primary dipole) but \sum' does not. Because the dipole moments of the ‘ghost’ dislocations and the primary dislocations are identical, the dipole–dipole interactions cancel and $E_{\text{dd}}(\mathbf{R}) - E_{\text{dg}}(\mathbf{R})$ represents a dipole–quadrupole interaction that decreases as R^{-3} with increasing R . Hence, the sum in equation (19) is absolutely convergent. This approach is similar to the fictitious charges introduced by Kudin and Scuseria (1998) to cancel the dipole corrections in the periodic lattice of electric dipoles. The validity of this solution is verified by comparing it with direct atomistic simulations in §4.2. The approach is also used to quantify and minimize the artificial image forces associated with dislocations in PBCs and to calculate dislocation Peierls stress in §4.3.

§4. APPLICATIONS

4.1. Atomistic modelling: introducing dislocations in the supercell

In this section, we consider the basic task of creating initial configurations for atomistic simulations of dislocation dipoles. At a first glance, there is no issue here since atomistic simulations of dislocations in PBCs have become commonplace. However, as discussed below, even in this relatively simple situation the problem of conditional convergence does exist. In some cases, subsequent relaxation of the initial atomic configuration takes care of the problem and eliminates the artefacts associated with the conditionally convergent lattice sums. However, the very same artefacts can be responsible for non-physical effects at the supercell boundaries that may persist through the subsequent atomistic simulations and could lead to uncontrollable errors if left unnoticed. This section discussed the nature of conditional convergence for the case of displacement fields in PBCs and describes a simple and efficient procedure for eliminating spurious misfit that is often created by introducing dislocations in the periodic supercells.

Let us consider a screw dislocation in the isotropic solid as an example. Assuming that it runs along z through the origin, its displacement field is

$$u_z(x, y) = b \frac{\theta}{2\pi}, \tag{20}$$

where θ is the angle between the position vector of the field point and a reference direction. Choice of the reference direction is arbitrary and amounts to fixing a mathematical cut plane across which the displacement field experiences a discontinuous jump by b . For example, choosing $\theta = \arctan(y/x)$ corresponds to a cut along the $-x$ axis. Figure 3(a) shows the displacement field $u_z^{\text{dipole}}(x, y)$ of a dislocation dipole with Burgers vector magnitude b positioned at $x = 0.5$, $y = 0$ and $-b$ at $x = -0.5$, $y = 0$, in a domain $x \in [-1, 1]$, $y \in [-0.5, 0.5]$. Clearly, $u_z^{\text{dipole}}(x, y)$ is not

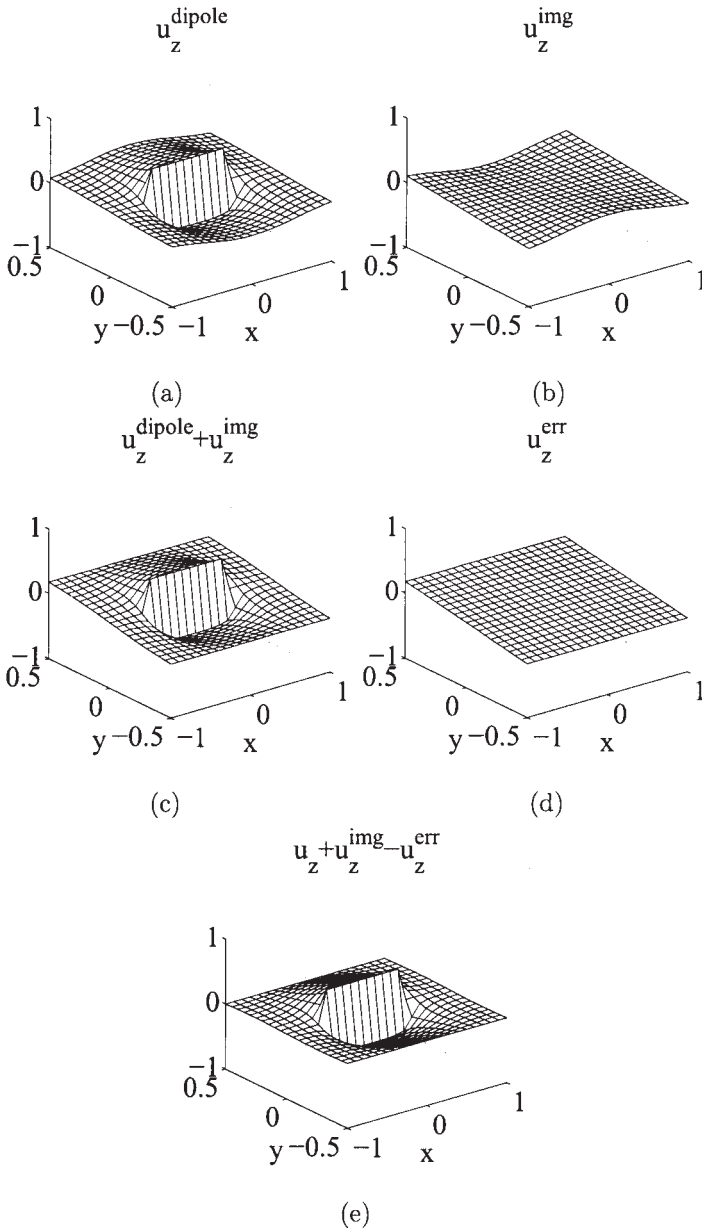


Figure 3. Constructing the displacement fields $u_z(x, y)$ of a screw dislocation dipole in PBCs by superimposing the displacement fields of (a) primary and (b) image dipoles. The superposition of (a) and (b) produces (c) a field that is not fully periodic. Only after (d) the error term is measured and subtracted, is (e) the expected periodicity restored.

periodic and may not be a good initial configuration for subsequent atomistic simulations.

In an attempt to generate the displacement field of a dislocation dipole that would satisfy the periodic boundary conditions, we superimpose the displacement fields of a periodic array of dipoles:

$$\mathbf{u}^{\text{sum}}(\mathbf{r}) = \sum_{\mathbf{R}} \mathbf{u}^{\text{dipole}}(\mathbf{r} - \mathbf{R}). \quad (21)$$

Figure 3(c) shows the result $\mathbf{u}^{\text{sum}}(\mathbf{r})$ of superposition of the displacement fields of dislocation dipoles within the rectangular box $|x| < 10$, $|y| < 5$. Figure 3(b) shows $\mathbf{u}^{\text{img}}(\mathbf{r}) \equiv \mathbf{u}^{\text{sum}}(\mathbf{r}) - \mathbf{u}^{\text{dipole}}(\mathbf{r})$, that is the displacement field generated by the image dipoles only, excluding the singular field of the primary dipole. We see that neither of the two fields is periodic.

Following the general discussion in §3, we trace the non-periodic component of the displacement field to the conditional convergence of the sum of the displacement fields of individual dipoles. That the two issues, conditional convergence and breaking of periodicity, are directly related is again confirmed by the fact that a unique solution for true displacement field can be obtained in two operationally different ways: firstly by direct regularization of the sum (equation (22)), by for example introducing ‘ghost’ dislocations around each image dipole, as in §3.2) and making it absolutely convergent; secondly, by summing a conditionally convergent sum and then subtracting the spurious components of the field thus obtained. Here, we choose the latter option, which we find is somewhat simpler to implement.

Considering that the displacement field of a dislocation dipole behaves as $1/r$ with increasing r , lattice sums of the second derivatives of the displacement field should be absolutely convergent. Hence, the conditional convergence can result, at worst, in a spurious linear term that depends on the order of summation or, for finite sums, on exactly how the summation is truncated:

$$\mathbf{u}^{\text{sum}}(\mathbf{r}) = \mathbf{u}^{\text{PBC}}(\mathbf{r}) + \mathbf{d} \cdot \mathbf{r} + \mathbf{u}^0. \quad (22)$$

Here, $\mathbf{u}^{\text{PBC}}(\mathbf{r})$ is periodic, \mathbf{d} is a constant tensor and \mathbf{u}^0 is a constant translation that can be eliminated by an appropriate choice of the coordinate origin. The linear component of the spurious field $\mathbf{u}^{\text{err}} \equiv \mathbf{d} \cdot \mathbf{r}$ can be readily evaluated by measuring the field at the cell corners. Depending on how many terms are summed to construct \mathbf{u}^{sum} , this term can be arbitrarily large and may manifest itself in artificial stacking faults due to displacement mismatch across the cell boundaries. To avoid such a possibility it is important to subtract this term. Figure 3(d) shows the spurious linear term \mathbf{u}^{err} while figure 3(e) shows the displacement field after subtracting \mathbf{u}^{err} . The resulting regularized field is fully periodic. This simple procedure is used throughout this paper to create initial structures for the atomistic simulations of dislocation dipoles.

In the above approach, it is important that the same set of image dipoles is used to compute the displacement field at all points within the primary cell. Alternatively, one can devise a slightly different summation procedure in which only the dipoles are summed whose centres fall into, say, a circle of fixed radius drawn around a given field point. Moving around in the primary supercell, the set of dipoles entering the partial sum will change when the boundary of the summation circle crosses the centre of a dipole. As a result, the sets of image dipoles contributing to each field point can be different. Interestingly, in this latter scheme, one always obtains a periodic field. Furthermore, numerical calculations show that, in the limit of large cut-off radius and without any further correction, this method usually generates a field that is almost identical with that obtained from the regularization procedure above. Similar observations have been reported by Wolf *et al.* (1999) in the context of electrostatic interactions. However, despite its simplicity, we cannot recommend

this method with conviction, since it is difficult to prove that it converges to the absolutely convergent physical solution. In fact, the field obtained in this way always contains discontinuities caused by sudden changes in the number of contributing image dipoles on going from one field point to another. At the same time, the regularization method discussed above always produces a smooth field that is also proven to be absolutely convergent.

4.2. Atomistic modelling: the core energy

In this section, we check the validity of equation (19) by comparing the energies of dislocation dipoles computed two ways: firstly, using a fully atomistic description of dislocations in PBCs and then using the linear elasticity solution developed in appendix A. We establish that the difference between the two energies does not depend on the supercell geometry, thus providing a consistent and physically meaningful way for extraction of the dislocation core energy through equation (6).

Figure 4 shows a screw dislocation dipole on the *shuffle-set* plane (Hirth and Lothe 1982, p. 376) in a periodic supercell with repeat vectors $\mathbf{c}_1 = 4[1\bar{1}\bar{2}]$, $\mathbf{c}_2 = 3[111]$ and $\mathbf{c}_3 = [1\bar{1}0]$. In this supercell, two dislocations are separated by $\mathbf{a} = \mathbf{c}_1/2$. To compute the interatomic forces we use the Stillinger–Weber (SW) (1985) potential model modified by Balamane *et al.* (1992). The elastic constants for the modified SW potential are $C_{11} = 161.6$ GPa, $C_{12} = 81.6$ GPa and $C_{44} = 60.3$ GPa. A dislocation dipole is initially introduced using the regularized elastic solution for the displacement field produced by a screw dislocation dipole in PBCs (see § 4.1 for details). Then, the forces between the atoms are relaxed using a conjugate gradient algorithm. In the relaxed configuration the atoms with local energies higher than the bulk cohesive energy by 0.08 eV are shown as full circles, to highlight the dislocation cores. Earlier, Koizumi *et al.* (2000) found that the SW model predicts two alternative core structures for the shuffle-set screw dislocations that are very close in energy. These two types were termed A and B. Both dislocations in figure 4(a) have cores of type A centring on the six-atom rings. On the other hand, two dislocations in figure 4(b) have cores of type B centring on the vertical bonds. Koizumi *et al.* (2000) reported that, of the two alternative core structures, core B has slightly lower energy in the SW model of silicon. We reproduce that result (see below) but note that an even earlier *ab initio* study (Arias and Joannopoulos 1994) reported core A as the ground state of the shuffle screw dislocation. We are currently exploring this issue using an *ab initio* framework and shall report our

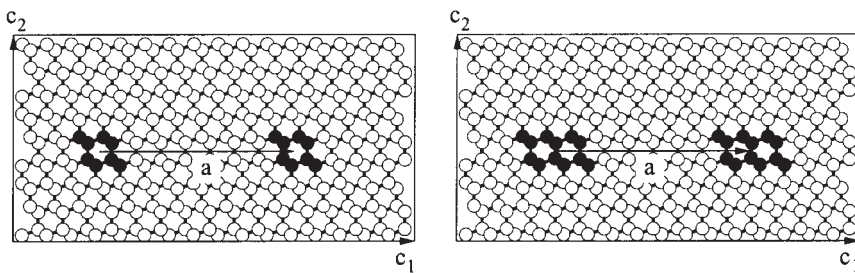


Figure 4. Atomic cell used for simulations of dislocations in silicon based on the SW potential (Balamane *et al.* 1992) with $\mathbf{c}_1 = 4[1\bar{1}\bar{2}]$, $\mathbf{c}_2 = 3[111]$ and $\mathbf{c}_3 = [1\bar{1}0]$. The cell contains a shuffle-set screw dislocation dipole with $\mathbf{a} = \mathbf{c}_1/2$. Dislocations core structures are of type A in (a) and type B in (b).

findings elsewhere. Here we focus solely on the comparison between the atomistic and elastic predictions for the energy of dislocation dipoles in PBCs.

First, we fix \mathbf{c}_2 and \mathbf{c}_3 but vary \mathbf{c}_1 , keeping $\mathbf{a} = \mathbf{c}_1/2$, to examine the agreement or lack thereof between the atomistic E_{atm} and elastic predictions for the dipole energies in PBCs. Figure 5(a) shows that E_{atm} varies linearly with c_1 with the same slope for both types of dislocation core: type A and type B. The core energy difference computed from these data is

$$E_{\text{core}}^A - E_{\text{core}}^B = 0.0375 \text{ eV } \text{\AA}^{-1}. \quad (23)$$

We then calculate elastic energies E_{el} for the same cell geometries. For consistency, we use the cubic elastic constants computed for the Balamane *et al.* (1992) version of the SW potential and employ the formula developed in appendix C for the dislocation interaction energy in a generally anisotropic solid. The results are plotted in figure 5 as open diamonds. The elastic energies also fall on to a straight line with a slope that agrees with the atomistic data to within 0.5%. This agreement between atomistic and elasticity results is significant, because there are no adjustable parameters in either calculation, in contrast to a previous study (Arias and Joannopoulos 1994). By subtracting E_{el} from E_{atm} , we obtain the core energies of the two structures: $E_{\text{core}}^A = 0.565 \pm 0.001 \text{ eV } \text{\AA}^{-1}$, and $E_{\text{core}}^B = 0.527 \pm 0.001 \text{ eV } \text{\AA}^{-1}$ at $r_c = b = 3.84 \text{ \AA}$. The core energies thus obtained are manifestly independent of \mathbf{c}_1 .

Having just obtained the core energies from the first series of supercell calculations, we confirm our results in a second series in which \mathbf{c}_1 is fixed at $4[11\bar{2}]$ but \mathbf{c}_2

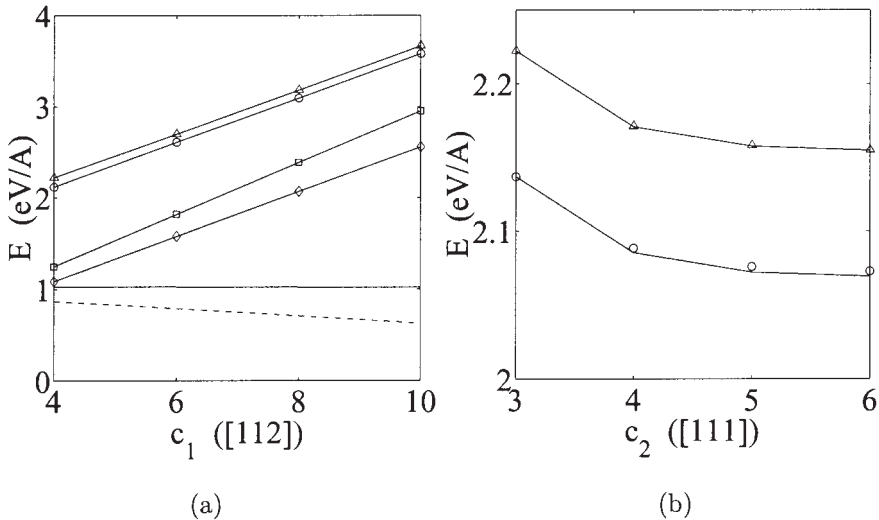


Figure 5. (a) Atomistic and linear elastic energies of the dislocation dipole computed in PBCs as functions of the supercell shape: (Δ), atomistic energies E_{atm}^A for core A; (\circ), atomistic energies E_{atm}^B for core B; (\diamond) elastic energy $E_{\text{el}}^{\text{aniso}}$ computed using anisotropic theory; (\square), elastic energy $E_{\text{el}}^{\text{iso}}$ computed by the isotropic elasticity; (—), $E_{\text{atm}}^B - E_{\text{el}}^{\text{aniso}}$; (---), $E_{\text{atm}}^B - E_{\text{el}}^{\text{iso}}$. (b) The total excess energy computed atomistically for $\mathbf{c}_1 = 3[11\bar{2}]$ and different \mathbf{c}_2 : (Δ), E_{atm}^A for core A, (\circ), E_{atm}^B for core B; (—), corresponding values obtained by summing the regularized anisotropic elastic energy with the core energies extracted from the data shown in (a).

varies from 3 to 6[111]. Figure 5(b) directly compares the atomistic data from this new series (open triangles and open circles) with the sum of the anisotropic elastic interactions plus $2E_{\text{core}}$ obtained from the data shown in figure 5(a) (solid lines). The agreement confirms that the use of the regularized lattice sums combined with a fully anisotropic treatment of elastic interactions provides a very reliable way to extract core energies from atomistic calculations. We notice that the agreement for type A dislocation is slightly better than that for type B, possibly owing to the compactness of core A.

An earlier calculation using an *ab initio* approach and the isotropic elasticity theory (Arias and Joannopoulos 1994) reported that $E_{\text{core}}^{\text{A}} = 0.56 \pm 0.21 \text{ eV } \text{\AA}^{-1}$ for the same $r_c = b = 3.84 \text{ \AA}$. Although the first-principles methods are generally more accurate than empirical potentials for predicting E_{atm} , anisotropic elasticity is considerably more accurate than isotropic elasticity for calculating E_{el} . To bring out the effects of elastic anisotropy, we repeated E_{el} calculations using isotropic elasticity. For that, elastic constants from the Voigt average (Hirth and Lothe 1982, p. 424) were used: shear modulus $\mu = 52.18 \text{ GPa}$ and Poisson's ratio $\nu = 0.2924$. The so-predicted elastic energies vary linearly with c_1 but the slope is 14% larger than for the atomistic data. In an attempt to 'improve' the isotropic elasticity estimate we replaced the shear modulus μ by an energy pre-factor $K = [C_{44}(C_{11} - C_{12})/2]^{1/2}$, as in the anisotropic expression for the dislocation self-energy (Ismail-Beigi and Arias 2000). However, the resulting slope is still too large by 8%. Alternatively one could treat μ as a free parameter to obtain a best fit with the atomistic data (Arias and Joannopoulos 1994). Such a procedure leads to a core energy of $E_{\text{core}}^{\text{B}} = 0.532 \pm 0.002 \text{ eV } \text{\AA}^{-1}$. Although this is rather close to our fully anisotropic prediction, the agreement may well be fortuitous. This is because fitting the slope using the isotropic formula for dislocation interactions amounts to trying to compensate one inaccuracy (the use of isotropic elasticity) by introducing another (specially fitted values of the isotropic elastic constants μ and ν). In our view, an accurate prediction of the core energetics should combine *ab initio* calculations with a fully anisotropic treatment of the elastic fields in PBCs.

4.3. Atomistic modelling: the Peierls stress

The third application of our regularization method is the computation of dislocation Peierls stress, that is the stress necessary to move a dislocation at zero temperature. Peierls stress is an important characteristic of the resistance to plastic deformation and correlates with the low temperature yield stress. Atomistic calculations of Peierls stress are often complicated by the image forces on dislocations associated with the boundary conditions. In this section we show that in PBCs the error associated with the image effects can be quantified and reduced with the help of elasticity calculations.

For Peierls stress calculations it is more convenient to position the dislocation dipole vertically, that is $\mathbf{a} = \mathbf{c}_2/2$. In this orientation, dislocations can glide on the horizontal planes and avoid recombination which would be inevitable for $\mathbf{a} = \mathbf{c}_1/2$. Here we report Peierls stress values computed for the more stable variant (type B) of the screw dislocation core in the SW model of silicon, because core A was observed to transform into core B under stress (Koizumi *et al.* 2000). We define x, y, z axes along $\mathbf{c}_1, \mathbf{c}_2, \mathbf{c}_3$ directions and apply stress σ_{yz} on the simulation cell using the Parrinello–Rahman (1981) implementation of the stress-controlled boundary condi-

tions. This stress exerts equal but opposite forces on the two dislocations of the dipole along x and $-x$ directions respectively. A critical stress is obtained in a series of calculations in which the applied stress is gradually increased. Each stress increment is followed by a complete relaxation of atomic forces, using a conjugate gradient algorithm. The critical stress τ_c is defined as the value of σ_{yz} at which continuous dislocation motion through the supercell sets in, manifesting itself in a failure of the conjugate gradient relaxation sequence to converge. Because of possible effects of the boundary image forces, τ_c is not necessarily equal to the Peierls stress τ_{PN} . The latter corresponds to a critical stress in an idealized situation, that is for a single dislocation in an infinite solid. Before presenting our results for τ_{PN} we examine, based on our regularization approach, the origin and the magnitude of the image forces in PBCs.

The image force is the negative derivative of the image energy with respect to the dislocation position. For our analysis it is useful to consider the variation of the total energy as a function of the relative position of two dislocations in the periodic supercell. Figure 6 shows the energy of a dislocation dipole computed atomistically under zero applied stress in PBCs, as a function of x , the distance between two dislocations along the \mathbf{c}_1 direction. The energy is seen to oscillate periodically, obviously owing to the interaction between two primary dislocations and their images. For comparison, plotted on the same graph is the elastic interaction energy computed for the same periodic supercell using the regularized anisotropic elasticity solutions presented in appendices A and C. The atomistic and the anisotropic elasticity energies agree very well. At the same time, the isotropic elasticity overestimates the magnitude of the oscillations by a factor of two, again indicating its inaccuracy in describing dislocation interactions.

Given the nearly perfect agreement between E_{atm} and E_{el} and the fact that the core energy does not affect the energy variations shown in figure 6, in the following we drop the subscripts atm and el and use a simpler notation E . The slope of the $E(x)$ curve in figure 6 is the image force that the dislocations see in addition to the

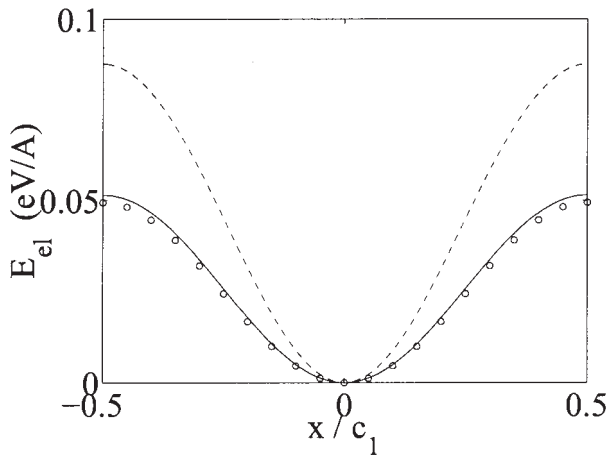


Figure 6. The energy (○) of a dislocation dipole in PBCs as a function of the relative position of two dislocations along the \mathbf{c}_1 direction and, when $x = 0$, two dislocations are separated by $\mathbf{a} = \mathbf{c}_2/2$: (—), anisotropic elasticity prediction; and (- - -), isotropic elasticity result.

Peach–Koehler force exerted by the external stress σ_{yz} . This extra force introduces an error in the Peierls stress value computed in PBCs. Considering the shape of the $E(x)$ curve, it becomes obvious that this error is minimized for dislocation positions where $dE/dx = 0$, that is either at $x = 0$ or at $x = c_1/2$. A second-order error still exists even in these two special configurations, owing to a finite curvature d^2E/dx^2 and the lattice discreteness. To examine the nature of this second-order effect let us define

$$\Delta E \equiv E(x = 0) - E\left(x = \frac{c_1}{2}\right). \quad (24)$$

If $\Delta E < 0$, as is the case for figure 6, then τ_c computed at $x = 0$ overestimates the Peierls stress, since the next lattice position has a slightly higher energy, owing to the positive curvature d^2E/dx^2 in this point. On the contrary, τ_c computed at $x = c_1/2$ will underestimate τ_{PN} . For situations when $\Delta E > 0$, the sign of this second-order error inverts. Below, we make use of these observations to devise a practical procedure for minimizing the error in Peierls stress calculations in PBC.

The elasticity theory predicts that ΔE is a homogeneous function of \mathbf{c}_1 , \mathbf{c}_2 and \mathbf{a} of degree 0. In other words, the elastic energy of the dislocation dipole in PBCs will not be affected by a simultaneous scaling of \mathbf{c}_1 , \mathbf{c}_2 and \mathbf{a} by the same numerical factor. Figure 7 shows this function for the shuffle-set screw dislocation dipole in SW silicon obtained from anisotropic (solid curve) and isotropic (broken curve) elasticity calculations for the rectangular supercells. Both functions asymptotically approach zero at very large ratios c_2/c_1 , that is when the cell becomes vertically elongated. However, the anisotropic solution predicts that $|\Delta E|$ also crosses zero at a finite ratio c_2/c_1 , whereas the isotropic solution decays monotonically with increasing c_2/c_1 . It is an interesting observation that implies that, if indeed ΔE becomes zero at some finite c_2/c_1 , a supercell can be designed to be as close to this special aspect ratio as

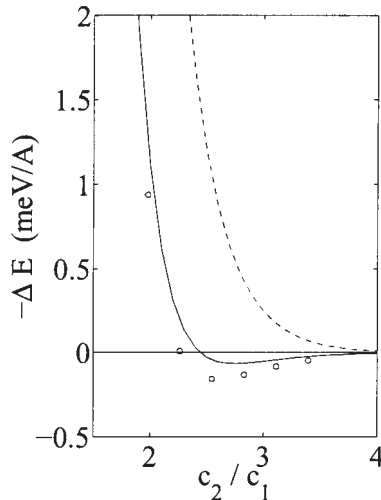


Figure 7. The amplitude ΔE of the energy variation as a function of the cell aspect ratio c_2/c_1 , for a shuffle-set screw dislocation dipole in silicon (Balamane *et al.* 1992). Anisotropic elasticity (—) predicts $\Delta E = 0$ at $c_2/c_1 = 2.5$. Isotropic elasticity (---) predicts a monotonic decrease in ΔE with increasing c_2/c_1 . Atomistic simulation data (○) with $\mathbf{c}_1 = 5[11\bar{2}]$ are also shown.

practically possible, to provide for cancellation of the image effects in the Peierls stress calculations. To explore this issue further, we performed a series of atomistic calculations for supercells with $\mathbf{c}_1 = 5[11\bar{2}]$ and $\mathbf{c}_2 = k[111]$. For the cell with $k = 16$, $|\Delta E|$ was found to be very small, only $0.9 \times 10^{-5} \text{ eV \AA}^{-1}$.

The existence of a special aspect ratio for which $\Delta E = 0$ is quite general. We have observed a similar behaviour for an edge dislocation dipole in bcc molybdenum (Cai *et al.* 2001), as shown in figure 8. Note the sign reversal of the y axis from figure 7. In this case the supercell repeat vectors \mathbf{c}_1 , \mathbf{c}_2 , \mathbf{c}_3 are along $[111]$, $[\bar{1}01]$ and $[1\bar{2}1]$ respectively, and $\mathbf{a} = \mathbf{c}_2/2$. The regularized anisotropic elasticity predicts that $|\Delta E|$ should vanish at $c_2/c_1 = 2.918$, whereas the isotropic solution again decays monotonically with increasing c_2/c_1 . To verify this prediction for the case of edge dipole in bcc Mo, we performed three sets of atomistic calculations with $\mathbf{c}_1 = 15, 20$ and $30[111]$ using the Finnis–Sinclair (1984) model. The results are largely consistent with the anisotropic elasticity prediction, but show a slight dependence on the supercell size. With increasing cell size the atomistic results seem to converge to the size-independent anisotropic elasticity solution, indicating that the latter describes the limiting behaviour when lattice discreteness becomes negligible.

Having examined the origin of error in Peierls stress calculations in PBCs, we are now well prepared to examine one lingering discrepancy reported in the literature. Using the same atomistic model, two groups reported two vastly different values for the Peierls stress of the shuffle-screw dislocations in silicon: 2.0 GPa in the paper by Koizumi *et al.* (2000) and 5.8 GPa in the paper by Ren *et al.* (1995). Figure 9(a) shows the critical stress τ_c computed for different c_2 with fixed $\mathbf{c}_1 = 5[11\bar{2}]$. Values of τ_c computed at $x = 0$ are shown as open triangles, while those computed at $x = c_1/2$ are plotted as open inverted triangles. Both sets of data converge to 1.98 GPa with

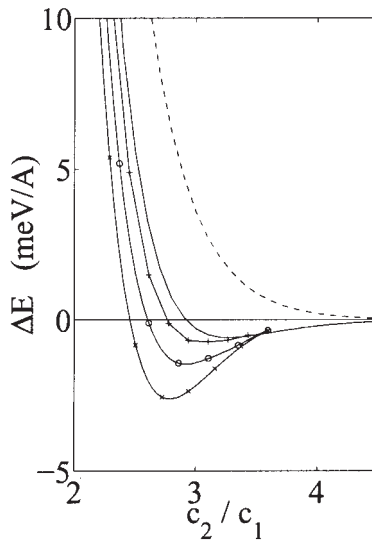


Figure 8. The amplitude ΔE of the energy variation as a function of the cell aspect ratio c_2/c_1 , for an edge dislocation dipole in bcc Mo (Finnis and Sinclair 1984). Anisotropic elasticity (—) predicts $\Delta E = 0$ at $c_2/c_1 = 2.918$. Isotropic elasticity (---) predicts that ΔE should decrease monotonically with increasing c_2/c_1 . Atomistic simulation data for $\mathbf{c}_1 = 15[111]$ (\times), $20[111]$ (\circ) and $30[111]$ ($+$) are shown.

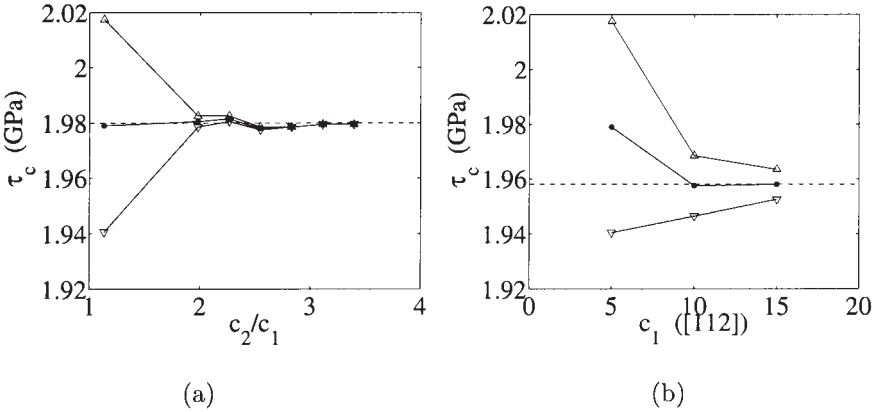


Figure 9. Critical stress to move a shuffle-set screw dislocations in silicon computed for (a) different c_2/c_1 with fixed $\mathbf{c}_1 = 5[11\bar{2}]$ and (b) different c_1 with fixed $c_2/c_1 = 1.1314$: (Δ), data points for $x = 0$; (∇), data points for $x = c_1/2$; (\bullet), obtained by averaging data points for $x = 0$ and $x = c_1/2$.

increasing c_2 , while their averaged values (full circles) reach this asymptotic value even for relatively short cells. It appears that the second-order error can be eliminated even for supercells with $c_2 \approx c_1$, by computing the critical stress for both high-symmetry positions $x = 0$ and $x = c_2/2$ and taking the average of two values. Given this observation, we now fix the aspect ratio at $c_2/c_1 = 1.1314$ and examine the convergence of τ_c with respect to the cell size. The results are shown in figure 9(b), for three different supercells with $\mathbf{c}_1 = 5[11\bar{2}]$, $10[11\bar{2}]$ and $15[11\bar{2}]$ and $\mathbf{c}_2 = 8[111]$, $16[111]$ and $24[111]$ respectively. The averaged τ_c are almost identical for $\mathbf{c}_1 = 10[11\bar{2}]$ and $15[11\bar{2}]$, converging to $\tau_{PN} = 1.96$ GPa. This value agrees with the more recent result of 2.0 GPa (Koizumi *et al.* 2000), prompting us to conclude that the earlier result of 5.8 GPa (Ren *et al.* 1995) is probably incorrect.

4.4. Stress field in three dimensions

This section focuses on yet another application of the regularization approach that is especially relevant for mesoscale dislocation dynamics simulations in three dimensions. In dislocation dynamics simulations, dislocation lines are discretized into short line segments (Devincre and Kubin 1997, Zbib *et al.* 1998, Schwarz 1999, Ghoniem *et al.* 2000), interacting with each other through long-range elastic fields. Numerical evaluation of these interactions presents a major computational bottleneck for dislocation dynamics simulations. The unit element of such calculations is evaluation of stress produced at a given material point P by a dislocation segment centred at position S. Using the analytical formulae developed in the continuum theory (Hirth and Lothe 1982, p. 132), it takes a few hundred arithmetic operations to obtain all six stress components from a general dislocation segment of finite length. If one were to use PBCs, the computational burden would increase manifold because the stress field of multiple periodic images of the primary segment would have to be evaluated. Considering that the overall computational burden of stress calculations already scales as $O(N^2)$ (here N is the number of dislocation segments) the brute-force treatment of the image stress in PBCs becomes prohibitive.

A possible solution (Bulatov *et al.* 2001) is to pre-calculate and tabulate the image stress, that is the correction stress due to the image segments, on a grid within the computational volume and then interpolate between the grid values during the simulations. Operationally, to calculate the tables, one needs to compute stress on grid points when the dislocation segment is located at the centre of the computational cell. Because only the stress fields of image segments that are outside the computational volume are summed, the correction stress is free of singularity and hence smooth. We only consider differential (point-like) dislocation segments, that is segments whose length $d\mathbf{l}$ is considerably smaller than their distance to the field point. Compared with the case of straight segments of finite length, the use of differential segments reduces the dimensionality of the tables from four to three. Furthermore, in the cubic simulation boxes, the total number of independent look-up tables can be reduced from 54 (six stress components \times nine components of tensor $\mathbf{b} \otimes d\mathbf{l}$) to eight by symmetry considerations. The remaining eight tables are for two stress components (σ_{12} and σ_{13}) for a unit screw segment $\mathbf{b} = d\mathbf{l} = [100]$ and for six stress components for a unit edge segment $\mathbf{b} = [010]$, $d\mathbf{l} = [100]$.

In the remaining part of this section, we consider an example of the stress σ_{13} produced by a differential edge segment in a unit simulation cube $x, y, z \in [-0.5, 0.5]$. Let us define $\sigma^{\text{seg}}(\mathbf{r})$ to be the stress field of a dislocation segment at the origin. In the isotropic elasticity (Hirth and Lothe 1982, p. 132),

$$\frac{\sigma_{13}^{\text{seg}}}{\mu} = \frac{\nu x}{(1-\nu)r^3} - \frac{3xz^2}{(1-\nu)r^5}, \tag{25}$$

where μ is the shear modulus, ν is Poisson's ratio and $r = (x^2 + y^2 + z^2)^{1/2}$. Define

$$\sigma^{\text{sum}}(\mathbf{r}) = \sum_{\mathbf{R}} \sigma^{\text{seg}}(\mathbf{r} - \mathbf{R}), \tag{26}$$

where the sum \sum runs over all lattice points in a three-dimensional sc lattice with the lattice constant equal to unity. The correction stress that we intend to tabulate excludes the primary dipole:

$$\sigma^{\text{img}}(\mathbf{r}) = \sigma^{\text{sum}}(\mathbf{r}) - \sigma^{\text{seg}}(\mathbf{r}) = \sum'_{\mathbf{R}} \sigma^{\text{seg}}(\mathbf{r} - \mathbf{R}), \tag{27}$$

where the sum \sum' excludes the origin.

Because $\sigma^{\text{seg}}(\mathbf{r}) \propto r^{-2}$ (equation (25)), the sum in equation (42) (now in three dimensions) is not absolutely convergent. However, the second derivatives of $\sigma^{\text{seg}}(\mathbf{r})$ scale as r^{-4} and their sum should be absolutely convergent. Similar to the case of displacement fields discussed in §4.3, the spurious field produced by the conditionally convergent sum is

$$\sigma^{\text{sum}}(\mathbf{r}) = \sigma^{\text{PBC}}(\mathbf{r}) + \mathbf{g} \cdot \mathbf{r} + \sigma^0, \tag{28}$$

where \mathbf{g} is a third-order tensor accounting for a stress gradient and σ^0 is an average stress. It is now straightforward to obtain a regularized solution $\sigma^{\text{PBC}}(\mathbf{r})$ from an arbitrarily chosen summation sequence $\sigma^{\text{sum}}(\mathbf{r})$, by measuring these two constants \mathbf{g} and σ^0 and subtracting them.

Because the stress fields of a differential dislocation segment should be anti-symmetric with respect to inversion, that is $\sigma^{\text{seg}}(-\mathbf{r}) = -\sigma^{\text{seg}}(\mathbf{r})$, it is a simple matter to ensure that $\sigma^0 = 0$ by always including the image segment at $-\mathbf{R}$ whenever an

image segment at \mathbf{R} is encountered. In other words, σ^0 vanishes if the following form for the stress field is assumed:

$$\sigma^{\text{sum}}(\mathbf{r}) = \frac{1}{2} \sum_{\mathbf{R}} \sigma^{\text{seg}}(\mathbf{r} - \mathbf{R}) + \sigma^{\text{seg}}(\mathbf{r} + \mathbf{R}). \quad (29)$$

The stress gradient \mathbf{g} , on the other hand, is generally non-zero. However, it can be easily calculated after the summation is completed, for example

$$\mathbf{g} \cdot \hat{e}_x = \sigma^{\text{sum}}\left(\frac{\hat{e}_x}{2}\right) - \sigma^{\text{sum}}\left(-\frac{\hat{e}_x}{2}\right), \quad (30)$$

and similarly for $\mathbf{g} \cdot \hat{e}_y$, $\mathbf{g} \cdot \hat{e}_z$, where \hat{e}_x is the unit vector along the x axis. The needed regularized solution is then

$$\sigma^{\text{PBC}}(\mathbf{r}) = \sigma^{\text{sum}}(\mathbf{r}) - \mathbf{g} \cdot \mathbf{r}. \quad (31)$$

As an example, we compute the stress field on a cubic $33 \times 33 \times 33$ grid within the unit cube. For that, we sum the contributions from all images within a larger cube $x, y, z \in [-20, 20]$. Figure 10 (a) shows σ_{13}^{sum} (in the units of μ for $\nu = 0.309$) as a function of x and y for fixed $z = 0.5$, before correction. We note that stress is not periodic along y direction. After the correction (equation (31)), the stress field becomes fully periodic, as shown in figure 10 (b). Figure 11 (a) shows an isosurface of the total (primary plus image) stress field computed for $\sigma_{13}^{\text{PBC}}(\mathbf{r}) = -2$; in this plot its singular behaviour at the origin and its periodicity along z direction are worth noticing. Figure 11 (b) shows an isosurface of the image stress for $\sigma_{13}^{\text{img}}(\mathbf{r}) = 0$, which is notably free of singularity and is zero at the origin. We also see that the correction field retains some periodicity and symmetry of the cube.

Two more plots of $\sigma_{13}^{\text{img}}(\mathbf{r})$ on planes $z = 0.5$ and $z = 0$ are shown in figures 12 (a) and (b) respectively. Here, it is interesting to note that the correction stress is generally non-zero on the cube faces. This observation calls into question the use of a cut-off distance for reducing the cost of computing the interactions between dislocation segments in dislocation dynamics simulations in three dimensions.

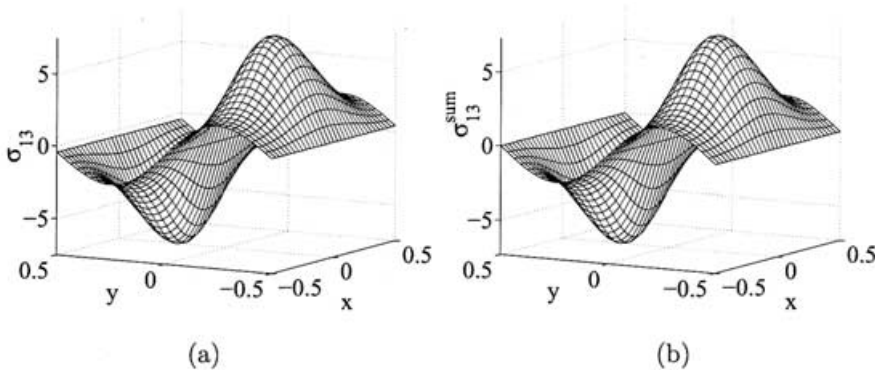


Figure 10. Stress field (xz component) of a differential edge dislocation segment in PBCs. σ_{13}^{sum} obtained by superimposing the stress field of a periodic array of segments, as a function of x and y at $z = 0.5$. Note that it is not fully periodic owing to a non-zero linear term. (b) The same, after subtracting the spurious linear term.

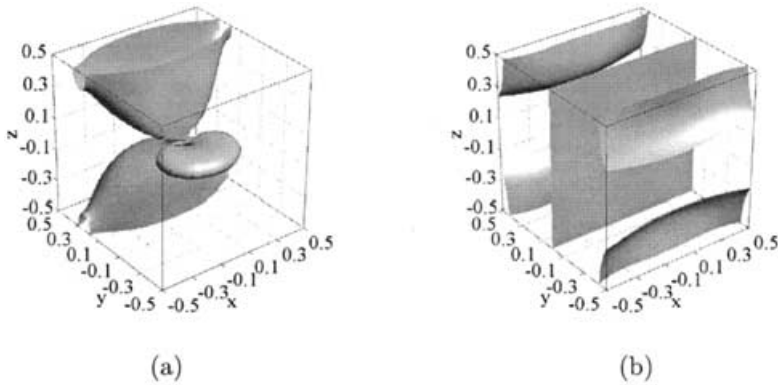


Figure 11. (a) Isosurface $\sigma_{13}^{\text{sum}} = -2$. (b) Zero-value isosurface of the tabulated stress correction term σ_{13}^{img} , interpolated in the unit cube as a function of segment position.

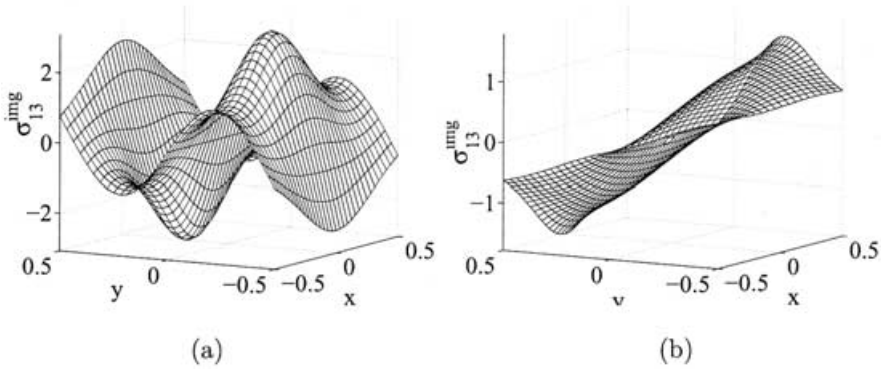


Figure 12. Correction stress field σ_{13}^{img} as a function of x and y ; (a) on plane $z = 0.5$; (b) on plane $z = 0$.

§ 5. SUMMARY

This contribution deals with the issue of conditional convergence of lattice sums of image interactions in periodic dislocation arrays. We examine the origin of the problem and show that conditional convergence produces spurious non-periodic fields that depend on the order of summation. Regularization of conditionally convergent sums can be achieved either by modifying each term in the sum in such a way that the new sequence becomes absolutely convergent, or by first computing a conditionally convergent sum and then correcting the result by subtracting the spurious field components. Given its operational convenience and the ease of implementation, in this work we mostly rely on the second approach. To check its applicability, we examine the method's performance in a variety of situations often encountered in dislocation modelling ranging from Peierls stress calculations in exceedingly small nanometre-sized supercells to large multiple micrometre-sized continuum simulations of dislocation dynamics. The results verify that the regularization techniques proposed here are accurate and robust.

ACKNOWLEDGEMENTS

This work was performed under the auspices of US Department of Energy by University of California Lawrence Livermore National Laboratory (LLNL) under contract No. W-7405-Eng-48. W.C. is supported by the Lawrence Postdoctoral Fellowship at LLNL. V.V.B. also acknowledges support from the Office of Basic Energy Sciences, US Department of Energy. The work of W.C., J.C. and S.Y. is partially supported by the LLNL under ASCI-Level 2 grant. S.Y. also acknowledges support by the US Air Force Office of Scientific Research (grant F49620-00-10082) and the National Science Foundation (grant DMR-9980015), and J.L. acknowledges support by Honda Research and Development.

 APPENDIX A
 DERIVATION OF THE IMAGE ENERGY

In this section, we first derive equation (15) for the total elastic energy of a dislocation dipole in a linear elastic medium under PBCs, by measuring the reversible work done to create the dipole. Then, by comparing the result with lattice sums of image interactions, we derive the correction term to the image energy computed through equation (17). Finally we express the correction term through ‘ghost’ dislocations and their interaction with the periodic array of image dipoles (equation (19)).

A.1. *Elastic energy of a dislocation dipole in periodic boundary conditions*

Consider a reversible path by which a dislocation dipole is inserted in a defect-free elastic medium under PBCs. Let E_1 be the energy of the medium before (initial state) and E_2 be the energy after the dipole is inserted (final state). For generality, let the initial state have a non-zero uniform stress σ^1 . Define E_0 as the energy of the defect-free and stress-free reference state. Then

$$E_1 = E_0 + \frac{1}{2} S_{ijkl} \sigma_{ij}^1 \sigma_{kl}^1 V \equiv E_0 + \frac{1}{2} S(\sigma^1)^2 V, \quad (\text{A } 1)$$

where S is the elastic compliance tensor and V is the volume of the periodic cell. The purpose of this section is to derive a useable expression for the total elastic energy $E_{\text{el}} = E_2 - E_0$ in terms of the stress field $\sigma(\mathbf{r})$ in the final state.

The energy difference $E_2 - E_1$ is obtained by calculating the reversible work done during insertion of the dislocation dipole. As shown in figure A 1, the dipole is created by making a cut along surface A , and displacing the sides of the cut with respect to each other by \mathbf{b} . To displace the cut surfaces, traction forces are applied to balance the additional internal stress that changes continuously from σ^1 to σ . Along the same path, the surface traction forces perform mechanical work

$$\begin{aligned} E_2 - E_1 &= \Delta W \\ &= -\frac{1}{2} \int dA_j b_i (\sigma_{ij}(\mathbf{r}) + \sigma_{ij}^1) \\ &= -\frac{1}{2} \int dA_j b_i \sigma_{ij}^0(\mathbf{r}) - \frac{1}{2} A_j b_i (\bar{\sigma}_{ij} + \sigma_{ij}^1), \end{aligned} \quad (\text{A } 2)$$

where $\bar{\sigma} \equiv \langle \sigma(\mathbf{r}) \rangle_V$ is the volume average of the final stress $\sigma(\mathbf{r})$, and $\sigma^0(\mathbf{r}) \equiv \sigma(\mathbf{r}) - \bar{\sigma}$ is the stress field variation around the average stress $\bar{\sigma}$.

We can now obtain E_{el} by summing equations (A 1) and (A 2) but wish to eliminate σ^1 and to express E_{el} solely in terms of $\bar{\sigma}$ and $\sigma^0(\mathbf{r})$ for our purposes. Note that creating the dislocation dipole introduces the plastic strain

$$\epsilon_{ij}^p = \left[\frac{b_i A_j}{V} \right]_s, \tag{A 3}$$

where the symmetrization is defined by $[a_{ij}]_s = (a_{ij} + a_{ji})/2$. Assuming that the boundaries of the periodic solid do not move in response to insertion of the dislocation dipole, the total average strain ϵ remains zero, that is

$$\epsilon_{ij} = \epsilon_{ij}^e + \epsilon_{ij}^p = 0, \tag{A 4}$$

$$\epsilon_{ij}^e = -\epsilon_{ij}^p = -\left[\frac{b_i A_j}{V} \right]_s, \tag{A 5}$$

where ϵ^e and ϵ^p are the average elastic and plastic strains respectively. The non-zero elastic strain produces a non-zero change in average stress associated with the dislocation dipole

$$\bar{\sigma}_{ij} - \sigma_{ij}^1 = C_{ijkl} \epsilon_{kl}^e = -C_{ijkl} \frac{b_k A_l}{V} \tag{A 6}$$

where $\mathbf{C} = \mathbf{S}^{-1}$ is the tensor of elastic constants. Therefore,

$$[b_i A_j]_s = S_{ijkl} V (\bar{\sigma}_{kl} - \sigma_{kl}^1), \tag{A 7}$$

$$b_i A_j (\bar{\sigma}_{ij} + \sigma_{ij}^1) = S_{ijkl} V (\bar{\sigma}_{ij} \bar{\sigma}_{kl} - \sigma_{ij}^1 \sigma_{kl}^1) \equiv SV [(\bar{\sigma})^2 - (\sigma^1)^2]. \tag{A 8}$$

Combining equation (A 1), (A 2) and (A 8), we have

$$E_{el} = E_2 - E_0 = -\frac{1}{2} \int dA_j b_i \sigma_{ij}^0(\mathbf{r}) + \frac{1}{2} S \bar{\sigma}^2 V. \tag{A 9}$$

The fact that σ_{ij}^1 drops out from the above equation is a restatement, for the case of periodic solid, of the theorem asserting that there is no interaction between external and internal stress in a linear elastic solid (Hirth and Lothe 1982, p. 53).

A.2. Correction term of image energy

In an attempt to relate equation (15) and the naïve image summation in equation (6), we write $\sigma^0(\mathbf{r})$ as a superimposition of the stress fields of image dislocation dipoles. Because $\langle \sigma_{ij}^0(\mathbf{r}) \rangle_V \equiv 0$ by definition, we have

$$\sigma_{ij}^0(\mathbf{r}) = \sigma_{ij}^{\text{sum}}(\mathbf{r}) - \sigma_{ij}^{\text{err}}, \tag{A 10}$$

$$\sigma_{ij}^{\text{sum}}(\mathbf{r}) \equiv \sum_{\mathbf{R}} \sigma_{ij}^{\text{dipole}}(\mathbf{r} - \mathbf{R}), \tag{A 11}$$

$$\sigma_{ij}^{\text{err}} \equiv \langle \sigma_{ij}^{\text{sum}}(\mathbf{r}) \rangle_V, \tag{A 12}$$

where $\sigma_{ij}^{\text{dipole}}(\mathbf{r} - \mathbf{R})$ is the stress field in \mathbf{r} produced by a dislocation dipole at \mathbf{R} and the summation \sum runs over all lattice sites $\mathbf{R} = n_1 \mathbf{c}_1 + n_2 \mathbf{c}_2$, with n_1 and n_2 integers, including $\mathbf{R} = \mathbf{0}$ (primary dipole). Note that the integration of the stress field produced by one dislocation dipole over the area enclosed by another dipole is simply the interaction energy between the two dipoles:

$$E_{\text{prm}} = -\frac{1}{2} \int dA_j b_i \sigma_{ij}^{\text{dipole}}(\mathbf{r}), \quad (\text{A } 13)$$

$$E_{\text{dd}}(\mathbf{R}) = - \int dA_j b_i \sigma_{ij}^{\text{dipole}}(\mathbf{r} - \mathbf{R}). \quad (\text{A } 14)$$

The factor $\frac{1}{2}$ in equation (A 13) accounts for self interaction. Substituting equations (A 10), (A 13) and (A 14) into equation (A 9), we obtain

$$E_{\text{el}} = E_{\text{prm}} + \frac{1}{2} \sum_R' E_{\text{dd}}(\mathbf{R}) + \frac{1}{2} A_j b_i \sigma_{ij}^{\text{err}} + \frac{1}{2} S \bar{\sigma}^2 V, \quad (\text{A } 15)$$

$$E_{\text{img}} = \frac{1}{2} \sum_R' E_{\text{dd}}(\mathbf{R}) + \frac{1}{2} A_j b_i \sigma_{ij}^{\text{err}} + \frac{1}{2} S \bar{\sigma}^2 V. \quad (\text{A } 16)$$

Assuming that the average stress $\bar{\sigma}$ in the periodic cell is zero, the correction term $\frac{1}{2} A_j b_i \sigma_{ij}^{\text{err}}$ is defined by the volume average of the lattice sum for the stress field σ_{ij}^{err} of primary and image dipoles. Interestingly, the lattice sum for $\frac{1}{2} A_j b_i \sigma_{ij}^{\text{err}}$ is also conditionally convergent but this term exactly cancels the error term in equation (6), provided that the same summation sequence is used to compute both sums. Therefore, the corrected E_{img} in equation (17) does not depend on the summation order and is absolutely convergent. This regularization procedure is similar to that used by Wolf (1992) for computing the Madelung sums of Coulomb interaction in the lattice of electric dipoles. The next section describes a convenient procedure for computing the correction term $\frac{1}{2} A_j b_i \sigma_{ij}^{\text{err}}$.

A.3. Potential field and ‘ghost’ dislocations

Since the average in equation (A 12) is not easy to compute, we provide a special procedure for computing $\frac{1}{2} A_j b_i \sigma_{ij}^{\text{err}}$ instead. We show that the correction term can be computed as a sum of interaction energies between the periodic array of dislocation dipoles and a set of test or ‘ghost’ dislocations.

Let L be the length of the cell along \mathbf{c}_3 (z direction). Then, as shown in figure A 1,

$$\mathbf{A} = (\mathbf{e}_z \times \mathbf{a})L, \quad \text{or,} \quad A_j = \epsilon_{j3k} a_k L \quad (\text{A } 17)$$

$$A_j b_i \sigma_{ij}^{\text{err}} = (\epsilon_{j3k} a_k L) b_i \sigma_{ij}^{\text{err}} = -a_k g_k L = -(\mathbf{a} \cdot \mathbf{g})L, \quad (\text{A } 18)$$

meaning that the correction term $A_j b_i \sigma_{ij}^{\text{err}}$ is proportional to the average slope \mathbf{g} of the potential field $\phi(\mathbf{r})$. Combining this with equation (14), and defining α, β to satisfy $\mathbf{a} = \alpha \mathbf{c}_1 + \beta \mathbf{c}_2$, we obtain

$$\begin{aligned} A_j b_i \sigma_{ij}^{\text{err}} &= -(\alpha \mathbf{c}_1 \cdot \mathbf{g} + \beta \mathbf{c}_2 \cdot \mathbf{g})L \\ &= -\{\alpha[\phi(\mathbf{r}_1 + \mathbf{c}_1) - \phi(\mathbf{r}_1)] + \beta[\phi(\mathbf{r}_2 + \mathbf{c}_2) - \phi(\mathbf{r}_2)]\}L. \end{aligned} \quad (\text{A } 19)$$

This equation points to a practical recipe for computing the correction term $A_j b_i \sigma_{ij}^{\text{err}}$. As shown in figure 1, we introduce four ‘ghost’ dislocations $\alpha \mathbf{b}$, $-\alpha \mathbf{b}$, $\beta \mathbf{b}$ and $-\beta \mathbf{b}$ such that $\alpha \mathbf{b}$ and $-\alpha \mathbf{b}$ are separated by \mathbf{c}_1 , and $\beta \mathbf{b}$ and $-\beta \mathbf{b}$ are separated by \mathbf{c}_2 . Defining $E_{\text{dg}}(\mathbf{R})$ to be the interaction energy between four ‘ghost’ dislocations and a dislocation dipole at \mathbf{R} , equation (A 19) can be rewritten as

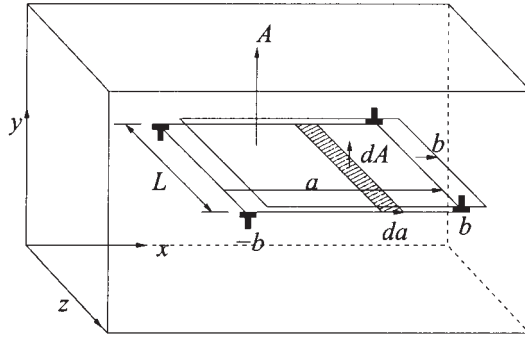


Figure A1. Introducing a dislocation dipole by cutting a defect-free medium along the surface **A** and displacing the positive side of the cut by **b** relative to the negative side.

$$A_j b_i \sigma_{ij}^{\text{err}} = - \sum_{\mathbf{R}} E_{\text{dg}}(\mathbf{R}), \tag{A 20}$$

$$\begin{aligned} E_{\text{img}} &= \frac{1}{2} \sum'_{\mathbf{R}} E_{\text{dd}}(\mathbf{R}) - \frac{1}{2} \sum_{\mathbf{R}} E_{\text{dg}}(\mathbf{R}) + \frac{1}{2} S \bar{\sigma}^2 V \\ &= \frac{1}{2} \sum'_{\mathbf{R}} [E_{\text{dd}}(\mathbf{R}) - E_{\text{dg}}(\mathbf{R})] - \frac{1}{2} E_{\text{dg}}(\mathbf{R} = 0) + \frac{1}{2} S \bar{\sigma}^2 V, \end{aligned} \tag{A 21}$$

in which \sum includes $\mathbf{R} = \mathbf{0}$ (primary dipole) but \sum' does not.

APPENDIX B

GREEN'S FUNCTION: AN ALTERNATIVE APPROACH TO ENERGY REGULARIZATION

The solution developed in §3 and appendix A is based on a derivation of the dislocation dipole energy in an elastic medium that is under PBCs. This energy (E_{cl}) was obtained by evaluating the work done along a reversible transformation path to the final state (dislocation dipole in PBCs) from some initial state with known energy. In that derivation, the initial state was chosen to be a defect free elastic solid under PBCs from which the final state was obtained by inserting a dislocation dipole through a cut and shift operation, under fixed PBCs. Given that the energy of the dislocated crystal under PBCs is a state variable, any other reversible transformation will work as well. For example, we can choose the initial state to be a dislocation dipole in an infinite elastic medium; the energy of this system is also known. The transformation is then on the boundary conditions, that is switching the infinite medium to a finite cell under PBCs. In this section, we briefly outline this procedure providing an alternative way to computing the image energy that is also free from the artefacts caused by conditional convergence.

Consider a dislocation dipole in an infinite elastic medium, as shown in figure B1(a), with elastic energy $E_1 = E_{\text{prm}}$ (e.g. equation (5)). Define B as the boundary of a parallelepiped box containing the dipole, and let $u(\mathbf{x})$ be the displacement field on B ($\mathbf{x} \in B$). Similar to the well-known Eshelby inclusion construct, let us carve out the box and exert a traction force $\mathbf{f}(\mathbf{x})$ on its border (and $-\mathbf{f}(\mathbf{x})$ on the inner surface of the hole in the infinite medium) to compensate for the internal stress that existed before carving the hole and to keep the displacement $\mathbf{u}(\mathbf{x})$ unchanged (figure B1(b)). The energy of transformation from this initial state to PBC can

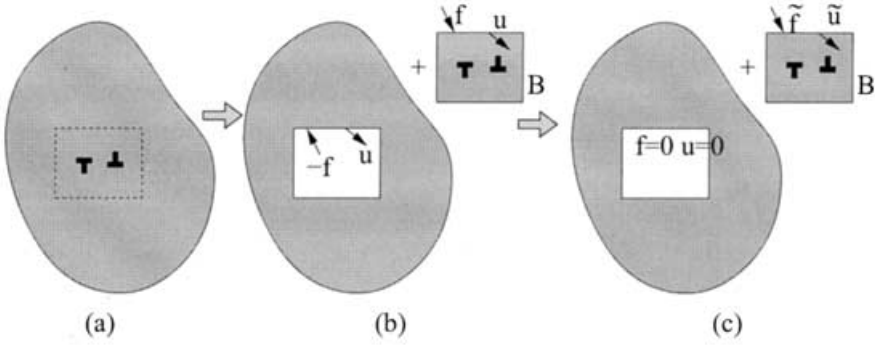


Figure B 1. A reversible path to transform the fields produced by (a) a dislocation dipole in an infinite medium into the fields of (c) a dipole contained in a periodic box. (b) The intermediate step in which the rectangular volume containing the dipole with boundary B is carved out and external forces \mathbf{f} and $-\mathbf{f}$ are exerted on the cut surfaces to maintain the displacement fields \mathbf{u} . The final configuration is obtained by relaxing the force tractions on the inner surfaces of the infinite domain and transforming \mathbf{f} and \mathbf{u} on the surfaces of the rectangular domain into $\tilde{\mathbf{f}}$ and $\tilde{\mathbf{u}}$ that satisfy PBCs.

now be obtained by summing two contributions (figure B 1 (c)): firstly, the energy stored in the infinite solid with the hole and, secondly, the energy required to deform the box to make it conform to periodic boundaries. The stored energy contribution is conveniently obtained by reducing the traction on the inner surface of the hole to zero and integrating the work performed along the way. At the same time, the energy of the additional deformation of the box to the required PBC shape can be obtained by changing the traction on the box surfaces from $\mathbf{f}(\mathbf{x})$ to $\tilde{\mathbf{f}}(\mathbf{x})$ and, simultaneously, changing $\mathbf{u}(\mathbf{x})$ to $\tilde{\mathbf{u}}(\mathbf{x})$ so that both $\tilde{\mathbf{f}}(\mathbf{x})$ and the resulting displacement on the boundaries both satisfy PBCs. The latter demand that $\tilde{\mathbf{u}}$ is symmetric and $\tilde{\mathbf{f}}$ is anti-symmetric on the opposite faces of B . Let the work done in these two transformations be ΔW_1 and ΔW_2 respectively, and define $\Delta \mathbf{f}(\mathbf{x}) \equiv \tilde{\mathbf{f}}(\mathbf{x}) - \mathbf{f}(\mathbf{x})$ and $\Delta \mathbf{u}(\mathbf{x}) \equiv \tilde{\mathbf{u}}(\mathbf{x}) - \mathbf{u}(\mathbf{x})$; then

$$E_{\text{img}} = \Delta W_1 + \Delta W_2, \quad (\text{B } 1)$$

$$\Delta W_1 = \frac{1}{2} \oint_B d\mathbf{x} \mathbf{f}(\mathbf{x}) \mathbf{u}(\mathbf{x}), \quad (\text{B } 2)$$

$$\Delta W_2 = \frac{1}{2} \oint_B d\mathbf{x} [\mathbf{f}(\mathbf{x}) + \tilde{\mathbf{f}}(\mathbf{x})] \Delta \mathbf{u}(\mathbf{x}). \quad (\text{B } 3)$$

Note that $\Delta \mathbf{f}(\mathbf{x})$ and $\Delta \mathbf{u}(\mathbf{x})$ are not independent but are related by

$$\Delta \mathbf{f}(\mathbf{x}) = \oint_B d\mathbf{x}' \mathbf{G}(\mathbf{x}, \mathbf{x}') \Delta \mathbf{u}(\mathbf{x}'), \quad (\text{B } 4)$$

where $\mathbf{G}(\mathbf{x}, \mathbf{x}')$ is the Green's function of the parallelepiped box bounded by B . Therefore,

$$\Delta W_2 = \frac{1}{2} \oint_B d\mathbf{x} \Delta \mathbf{u}(\mathbf{x}) \cdot \left(2\mathbf{f}(\mathbf{x}) + \oint_B d\mathbf{x}' \mathbf{G}(\mathbf{x}, \mathbf{x}') \Delta \mathbf{u}(\mathbf{x}') \right). \quad (\text{B } 5)$$

Given that $\mathbf{f}(\mathbf{x})$ and $\mathbf{u}(\mathbf{x})$ are known from the solution of a dislocation dipole in an infinite medium, ΔW_2 and hence E_{img} can be obtained by finding the $\Delta \mathbf{u}(\mathbf{x})$ that minimizes equation (B 5) under the constraint that $\tilde{\mathbf{u}}$ is symmetric and $\tilde{\mathbf{f}}$ is anti-symmetric on the opposite faces of boundary B .

We have developed a finite-element-model-based numerical procedure that minimizes equation (B 5) under the periodic boundary constraints. The procedure is found to produce numerical results that are identical with the results obtained using the ‘ghost’ dipole regularization procedure described in §3 and appendix A. Given that the latter is simpler to implement, we used the ‘ghost’ dislocation method in this work almost exclusively.

APPENDIX C

DISLOCATION INTERACTION IN ANISOTROPIC ELASTICITY

This appendix provides a useful formula for the interaction energy between two parallel straight dislocations in a generally anisotropic elastic medium. This energy is obtained by integrating the force exerted by a dislocation at the origin on another dislocations at (x, y) (the dislocations are assumed to be parallel to z axis).

The stress field of a dislocation (Burgers vector $\mathbf{b}^{(1)}$) at the origin is given by the well-known Stroh solution (Hirth and Lothe 1982, p. 436):

$$\sigma_{ij} = \text{Re} \left(\frac{-1}{2\pi i} \sum_{n=1}^3 B_{ijk}(n) A_k(n) \mathbf{D}(n) \eta_n^{-1} \right), \tag{C 1}$$

where $\eta_n = x + p_n y$, $n = 1, 2, 3, 4, 5, 6$ and p_n are the roots of the sextic equation (Hirth and Lothe 1982, p. 436) and $p_4 = p_1^*$, $p_5 = p_2^*$, $p_6 = p_3^*$. \mathbf{B} , \mathbf{A} and \mathbf{D} are certain tensors of rank 3, 1, 0 that depend on the elastic constants and p_n and $\mathbf{b}^{(1)}$. According to the Peach–Koehler equation the force per unit length of the second dislocation (Burgers vector $\mathbf{b}^{(2)}$) is

$$\mathbf{f} = (\boldsymbol{\sigma} \cdot \mathbf{b}^{(2)}) \times \hat{\mathbf{e}}_z. \tag{C 2}$$

Define

$$h_\beta(n) = \epsilon_{j3\beta} B_{ijk}(n) b_i^{(2)} A_k(n) \mathbf{D}(n), \quad \beta = 1, 2. \tag{C 3}$$

Then

$$f(x, y) = \sum_{n=1}^3 \text{Re} \left(\frac{-1}{2\pi i} \frac{h_\beta(n)}{x + p_n y} \right). \tag{C 4}$$

Defining the polar coordinates (r, θ) as shown in figure C 1, one has $x = r \cos \theta$, $y = r \sin \theta$. Taking $(r = r_c, \theta = 0)$ as the reference state in which the interaction energy $W = 0$, the energy W at any point along the x axis can be obtained by straightforward integration:

$$W(r, \theta = 0) = - \int_{r_c}^r \mathbf{f} \cdot d\mathbf{r} = \sum_{n=1}^3 \text{Re} \left[\frac{1}{2\pi i} h_1(n) \ln \left(\frac{r}{r_c} \right) \right]. \tag{C 5}$$

Now, the required energy $W(r, \theta)$ can be obtained by integrating along the arc with constant r , as in figure C 1 (b), that is

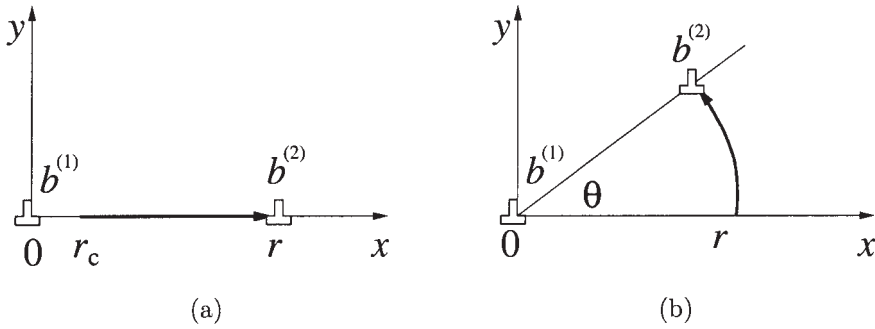


Figure C1. Integration path for computing the work done on moving the second dislocation $b^{(2)}$ at \mathbf{r} , in the stress field of the first dislocation $b^{(1)}$, at the origin. (a) Dislocation $b^{(2)}$ is moved along x axis from the reference position r_c to r . (b) Dislocation $b^{(2)}$ is moved along a circular arc θ while its distance from the first dislocation remains unchanged.

$$W(r, \theta) - W(r, 0) = - \int_0^\theta r d\theta \mathbf{f} \cdot \hat{\mathbf{e}}_\theta = \sum_{n=1}^3 \operatorname{Re} \left(\frac{1}{2\pi i} h_1(n) \ln(\cos \theta + p_n \sin \theta) \right). \quad (\text{C } 6)$$

This second integration uses the fact that $h_2(n) = h_1(n)p_n$, which can be proven by demanding the total work to be zero when the second dislocation moves along a closed path $(x_0, 0) \rightarrow (x, 0) \rightarrow (x, y) \rightarrow (x_0, y) \rightarrow (x_0, 0)$. The final result is then

$$W(r, \theta) = \sum_{n=1}^3 \operatorname{Re} \left\{ \frac{1}{2\pi i} h_1(n) \left[\ln \left(\frac{r}{r_c} \right) + \ln(\cos \theta + p_n \sin \theta) \right] \right\}, \quad (\text{C } 7)$$

$$W(x, y) = \sum_{n=1}^3 \operatorname{Re} \left[\frac{1}{2\pi i} h_1(n) \ln \left(\frac{x + p_n y}{r_c} \right) \right]. \quad (\text{C } 8)$$

REFERENCES

- ARIAS, T. A., and JOANNOPOULOS, J. D., 1994, *Phys. Rev. Lett.*, **73**, 680.
 BALAMANE, H., HALICIOGLU, T., and TILLER, W. A., 1992, *Phys. Rev. B*, **46**, 2250.
 BIGGER, J. R. K., MCINNES, D. A., SUTTON, A. P., PAYNE, M. C., STICH, I., KING-SMITH, R. D., BIRD, D. M., and CLARKE, L. J., 1992, *Phys. Rev. Lett.*, **69**, 2224.
 BLASE, X., LIN, K., CANNING, A., LOUIE, S. G., and CHRZAN, D. C., 2000, *Phys. Rev. Lett.*, **84**, 5780.
 BORWEIN, D., BORWEIN, J. M., and TAYLOR, K. F., 1985, *J. math. Phys.*, **26**, 2999.
 BULATOV, V. V., RHEE, M., and CAI, W., 2001, *Mater. Res. Soc. Symp.*, **653**, Z1.3.1.
 CAI, W., 2001, PhD Thesis, Massachusetts Institute of Technology, Cambridge, Massachusetts, USA.
 CAI, W., and BULATOV, V. V., CHANG, J., LI, J., YIP, S., 2001, *Phys. Rev. Lett.*, **86**, 5727.
 DE LEEUW, S. W., PERRAM, J. W., and SMITH, E. R., 1980, *Proc. R. Soc. A*, **373**, 27, 57.
 DEVINCERE, B., and KUBIN, L. P., 1997, *Mater. Sci. Engng*, **A8**, 234.
 FINNIS, M. W., and SINCLAIR, J. E., 1984, *Phil. Mag. A*, **50**, 45.
 GHONIEM, N. M., TONG, S.-H., and SUN, L. Z., 2000, *Phys. Rev. B*, **61**, 913.
 GULLUOGLU, A. N., SROLOVITZ, D. J., LESAR, R., and LOMDAHL, P. S., 1989, *Scripta metall.*, **23**, 1347.
 HANSEN, L. B., STOKBRO, K., LUNDQVIST, B. I., JACOBSEN, K. W., and DEAVEN, D. M., 1995, *Phys. Rev. Lett.*, **75**, 4444.
 HIRTH, J. P., and LOTHE, J., 1982, *Theory of Dislocations* (New York: Wiley).
 ISMAIL-BEIGI, S., and ARIAS, T. A., 2000, *Phys. Rev. Lett.*, **84**, 1499.
 KITTEL, C., 1976, *Introduction to Solid State Physics* (New York: Wiley).

- KOIZUMI, H., KAMIMURA, Y., and SUZUKI, T., 2000, *Phil. Mag. A*, **80**, 609.
- KUDIN, K. N., and SCUSERIA, G. E., 1998, *Chem. Phys. Lett.*, **283**, 61.
- LEHTO, N., and HEGGIE, M. I., 1999, *Properties of Crystalline Silicon*, edited by R. Hull (London: INSPEC), pp. 357–378.
- PARRINELLO, M., and RAHMAN, A., 1981, *J. appl. Phys.*, **52**, 7182.
- REN, Q., and JOOS, B., Duesbery, M. S., 1995, *Phys. Rev. B*, **52**, 13 223.
- SCHWARZ, K. W., 1999, *J. appl. Phys.*, **85**, 108.
- SMITH, E. R., 1981, *Proc. R. Soc. A*, **375**, 475.
- STILLINGER, F. H., and WEBER, T. A., 1985, *Phys. Rev. B*, **31**, 5262.
- WANG, H. Y., and LESAR, R., 1995, *Phil. Mag. A*, **71**, 149.
- WHITTAKER, E. T., and WATSON, G. N., 1958, *A Course of Modern Analysis* (Cambridge University Press).
- WOLF, D., 1992, *Phys. Rev. Lett.*, **68**, 3315.
- WOLF, D., KEBLINSKI, P., PHILLPOT, S. R., and EGGBRECHT, J., 1999, *J. chem. Phys.*, **110**, 8254.
- ZBIB, H. M., RHEE, M., and HIRTH, J. P., 1998, *Int. J. mech. Sci.*, **40**, 11.

